ELSEVIER

Carbohydrate Polymers 44 (2001) 217–231

Carbohydrate Polymers

www.elsevier.com/locate/carbpol

Steady shear and transient properties of starch in dimethylsulfoxide

B. Kapoor*, M. Bhattacharya

Department of Biosystems and Agricultural Engineering, University of Minnesota, St. Paul, MN 55108, USA

Received 29 December 1999; revised 13 April 2000; accepted 13 April 2000

Abstract

The effect of starch composition (amylose to amylopectin ratio) and concentration (2, 4, 6, and 8%) on the steady shear (η), transient ($G(t)$, $\eta^+(\dot{\gamma},t)\eta^-(\dot{\gamma},t)$, and $J(t)$) properties of starch in a mixed solvent (10% water-90% DMSO) was investigated. High amylose corn starch containing 70% amylose and 30% amylopectin, common corn starch containing 25% amylose and 75% amylopectin, and waxy corn starch containing about 99% amylopectin were the three starch types used. Changes in the concentration or the amylose to amylopectin ratio in the starch changed the behavior from Newtonian liquid to semidilute solution to viscoelastic solid. Shear thinning occurred at lower shear rate with increasing concentration. Time-strain separability was found to be applicable for concentrations of 2 and 4% and stresses were found to relax monotonically to zero. Waxy corn starch at higher concentration (6 and 8%) had a high magnitude of recovered strain typical of gels. High amylose corn starch samples were in the semi-dilute concentration regime. A single integral constitutive equation (K-BKZ) was proposed to model rheological data for 2, 4, and 6% common corn starch, and 2 and 4% waxy corn starch and gave an acceptable fit to the data. A more complex behavior was observed for 8% common corn starch and 6 and 8% waxy corn starch, with changes in network structure manifested in the lack of reproducibility of data.

Keywords: Biodegradable polymers; Steady shear and transient properties; Rheological properties; Starch

1. Introduction

The use of natural and biodegradable polymers has increased due to a growing awareness of environmental concerns and depleting oil reserves. Starch is a reserve polysaccharide substance occurring naturally as minute granules (2–100 μm particle size) in the roots, seeds, and stems of several types of plants including rice, wheat, barley, tapioca, millet, corn, and potatoes. Starch is a blend of two polymers, amylose and amylopectin, containing D-glucopyranosyl residues which differ with respect to glucopyranosyl linkage. Amylopectin is a highly branched molecule containing a mixture of α-1,4-D-glucose and α-1,6-D-glucose linkages with molecular weight in the millions. Amylose is a linear molecule with a α-1,4-D-glucose linkages and a molecular weight in the hundreds of thousands. Starch granules have a complex packing arrangement of the two constituent polymers, which has not been established conclusively. Granule size, shape, and composition (i.e. amylose/amylopectin content) vary with the plant source. Small amounts of non-carbohydrate components like lipids, proteins, and ash are also present (Whistler & Daniel, 1984; Young, 1984).

Apart from its use in foods, starch and its derivatives have been used in the formulation of products for adhesives, detergents, ceramics, polishes, explosives, paper coatings, aids in textile industry, and in oil recovery operations. Significant progress in the chemical and enzymatic syntheses and modifications of polysaccharides has extended the range of their applications. Both amylose and amylopectin have been synthesized using enzymes (Lapasin & Pricl, 1995). New methods for the chemical modification of polysaccharide chains are the focus of current research in order to derive products with "tailor-made" characteristics for a variety of applications. Homogeneous processes using organic solvents can be used to obtain derivatives from native starch with uniform and selective substitution (Lapasin & Pricl, 1995; Wurzburg, 1986). The mixed solvent system, water-dimethyl sulfoxide (DMSO), has been used as a solubilizing agent for starch and its components (Dintzis & Tobin, 1969). DMSO and DMSO-water system is the solvent of choice for most modified starches (Wurzburg, 1986). However, there is limited data available on the rheology of starch-aqueous DMSO systems.

There have been studies reported in the literature on the rheological properties of native starch solubilized using

* Corresponding author. Applied Materials, 3330 Scott Blvd., M/S 0681, Santa Clara, CA 95054, USA.

0144-8617/01/$ - see front matter
PII: S0144-8617(00)00218-6

90% DMSO-10% water (Dintzis & Bagley, 1995a,b; Dintzis, Berhow & Bagley, 1996). Shear-thickening, quasihysteresis loops of shear stress vs shear rate, and a flow-induced structure were observed for a 2% (w/v) solution of Amioca, a waxy starch, while common corn starch did not exhibit such phenomena (Dintzis & Bagley, 1995a; Dintzis et al., 1996). The observed phenomena were dependent on the method of solubilizing the starch. Increasing the severity of the processing method by increasing the time of stirring led to the phenomena of shear thickening and quasihysteresis loops not being observed. It was also reported that the distribution of the starch components might not be uniform in the waxy starch-aqueous DMSO liquid systems that exhibited shear thickening (Dintzis & Bagley, 1995a). The effect of thermomechanical processing on the viscosity behavior of corn starches has been reported (Dintzis & Bagley, 1995b). The intrinsic viscosity of the solutions decreased with increasing severity of the treatment (Dintzis & Bagley, 1995b).

This study focuses on the rheological characterization of starch dispersed in aqueous DMSO in order to understand the structure and flow behavior. Generally, knowledge of rheological properties is sought for better analysis of existing processes. However, such data could also be used to identify new applications for a particular material. This work attempts to provide an analysis as well as a model for the viscoelastic behavior of a physically crosslinked system. This information would be useful in both prediction of flow properties in existing processes (where starch in organic solvents is used), as well as finding new applications for starch in organic solvents.

The objective and purpose of this paper is to provide a quantitative analysis for the power-law behavior observed in a physically crosslinking system and compare with observations reported earlier in the literature, as well as theory, e.g. dynamic scaling theory.

2. Experimental procedure

2.1. Materials

Three types of native starches with different compositions were obtained from the American Maize Products Company. The approximate compositions were known (Delgado, Gottnied & Ammeraal, 1991). Amylomaize VII, a high amylose starch, contained about 70% amylose and 30% amylopectin. Amioca, a waxy starch, contained about 99% amylopectin. Common corn starch contained about 75% amylopectin and 25% amylose. The moisture content of each type of starch was estimated to be about 10% weight by weight basis.

Certified grade DMSO with water content less than 0.2% was obtained from Fisher Scientific. Water used was purified using the Millipore reverse osmosis system.

2.2. Sample preparation

Weighted amounts of starch were mixed with a 90% (v/v) solution of DMSO with water using a spatula till a milky white suspension was obtained. This usually took about one minute of stirring. A stirrer bar was put in the beaker which was covered with aluminum foil and placed in a water bath at about 96–98°C. This corresponded to a sample temperature of approximately 85–87°C. The beaker was heated with stirring for 15 min at 50 rpm, after which stirring was stopped and the beaker heated for an additional 15 min. The milky white suspension became clear as the starch gelatinized and solubilized. It was then cooled to room temperature and loaded in the rheometer. The effect of storage time of the samples prior to loading in the rheometer was determined by testing samples of the same concentration with different storage times.

Concentrations of 2, 4, 6, and 8% (w/v) of each starch dissolved in aqueous DMSO (90% DMSO, 10% water) were used in the rheological study. In this work, concentration units are % (w/v) unless otherwise mentioned. The beaker containing the solutions was weighed before and after the heating experiments to ensure against any water loss.

2.3. Rheological measurements

Rheometers capable of measuring material functions in shear deformation are derived from two basic designs, either controlled strain or controlled stress. The advantages and disadvantages of the two designs have been summarized (Macosko, 1994). Controlled strain instruments have better response at short time for low viscosity materials. Controlled stress is often a natural loading, is more sensitive to material changes, and allows the determination of a yield stress, if applicable. Both strain and stress controlled instruments were used to probe viscoelastic behavior.

A Rheometrics Fluids Spectrometer (RFS-II) manufactured by Rheometrics Inc., Piscataway NJ, was the strain-controlled rheometer used. The apparatus consisted of a rotating outer cylinder (cup) into which the sample was initially transferred. The inner cylinder (bob) was suspended from an air bearing and torque measured using transducers in the range 0.002–100 g cm. The diameters of the cup and bob were 34 and 32 mm, respectively, and the bob length was 33 mm. Temperature control (in the range ~10–90°C) was achieved by using a circulating fluid bath. The apparatus can measure both steady shear and dynamic flow properties for fluids having viscosities in the range $\sim 10^{-3}$–10^{5} Pa s.

The working equations for the couette geometry have been derived using the assumptions of steady, laminar, isothermal flow and negligible gravity and end effects. The equations of motion can then be solved to get the expression for shear stress on the inner cylinder for the

case of rotating outer cylinder as

$$\tau_{r\theta} = \frac{M_i}{2\pi R_i^2 L} \tag{1}$$

where M_i is the torque measured on the inner cylinder, R_i and L are the radius and length of the inner cylinder, respectively.

A Dynamic Stress Rheometer (DSR) manufactured by Rheometrics Incorporated was used to study material behavior at long times. Couette geometry was used with the diameters of the cup and bob 32 and 29.5 mm, respectively, and a bob length of 44.2 mm. The DSR is a controlled stress rheometer, where stress is applied by a drag cup motor, which is a rotary actuator attached to a precision air bearing. A position sensor using an optical encoder mounted on the stress head outputs strain, the angular deflection of the stress head. The analysis of applied stress and resulting strain leads to the calculation of the material properties. Instrument inertia is the major limitation and dominates with low viscosity samples (Krieger, 1990). A correction for instrument inertia is attempted by the instrument software. However, corrections for step changes in torque such as at the start-up of creep and recovery and at high frequencies ($\omega > 50$ rad/s) during sinusoidal oscillations are difficult (Macosko, 1994). The effect of inertia on the data obtained at short time during creep and recovery measurements was observed.

All samples were loaded at room temperature and allowed to equilibrate for about 15 min. This was done to allow temperature equilibration and stress relaxation. All the rheological measurements were carried out at 21–23°C.

2.4. Modeling of material functions

Bernstein, Kearsley and Zapas (1963), and independently Kaye (1962), proposed a single integral constitutive equation of the form

$$\tau_{ij} = \int_{-\infty}^{t} 2\left[\frac{\partial u(\mathrm{I}_B, \mathrm{II}_B, t-t')}{\partial \mathrm{I}_B} B_{ij}(t-t') - \frac{\partial u(\mathrm{I}_B, \mathrm{II}_B, t-t')}{\partial \mathrm{II}_B} B_{ij}^{-1}(t,t') \right] \mathrm{d}t' \tag{2}$$

where $u(\mathrm{I}_B, \mathrm{II}_B, t–t')$ is a time dependent elastic energy kernel function, $B_{ij}(t,t')$ is the Finger tensor, I_B and II_B are the first and second invariant of the Finger tensor. The K-BKZ equation can be simplified using the concept of time-strain factorability proposed by Wagner (1976a,b) to yield the factorized K-BKZ equation

$$\tau_{ij} = \int_{-\infty}^{t} 2M(t-t') \times \left[\frac{\partial U(\mathrm{I}_B, \mathrm{II}_B)}{\partial \mathrm{I}_B} B_{ij}(t,t') - \frac{\partial U(\mathrm{I}_B, \mathrm{II}_B)}{\partial \mathrm{II}_B} \mathrm{B}_{ij}^{-1}(t,t') \right] \mathrm{d}t' \tag{3}$$

Here $M(t–t')$ is the memory function which can be obtained from linear viscoelastic experiments, and $U(\mathrm{I}_B, \mathrm{II}_B)$ is the strain-energy function to be obtained from nonlinear viscoelastic experiments. The Rivlin–Sawyers equation is the most general constitutive equation for isotropic fluids and includes the K-BKZ equation (Bird, Armstrong & Hassager, 1987). The factorized Rivlin–Sawyers equation is given as

$$\tau_{ij} = \int_{-\infty}^{t} M(t-t')[\phi_1(\mathrm{I}_B, \mathrm{II}_B) B_{ij}(t,t') + \phi_2(\mathrm{I}_B, \mathrm{II}_B) B_{ij}^{-1}(t,t')]\, \mathrm{d}t' \tag{4}$$

Here ϕ_1 and ϕ_2 are the kernel functions and are not necessarily derivatives with I_B and II_B of a strain-energy function (Macosko, 1994). Several forms for the kernel functions have been proposed, and a compilation can be found in books by Bird and coworkers (Bird et al., 1987 and Macosko, 1994). Polymers for which time-strain separability has been reported to hold experimentally include Melt I, a low-density polyethylene having a broad molecular weight distribution (Laun, 1978), commercial polystyrene and polyethylene melts (Soskey & Winter, 1983), polydimethylsiloxanes (Papanastasiou, Scriven & Macosko, 1983), and a commercial polydisperse linear low-density polyethylene (Larson, 1985a).

Papanastasiou et al. (1983) have used kernel functions of the form

$$\phi_1(\mathrm{I}_B, \mathrm{II}_B) = \frac{1}{1 + a(\mathrm{I}_B - 3) + b(\mathrm{II}_B - 3)}$$

$$\phi_2(\mathrm{I}_B, \mathrm{II}_B) = 0 \tag{5}$$

to model viscoelastic behavior of two polydimethylsiloxanes in both shear and extension. Larson (1985a,b) observed a power-law relaxation modulus (see Eq. (13)) for a polydisperse linear low-density polyethylene. Utilizing the applicability of time-strain separability, nonlinear viscoelasticity in shear was modeled by a factorized K-BKZ equation of the form

$$\tau_{ij} = \int_{-\infty}^{t} M(t-t') h(\gamma) B_{ij}(t,t')\, \mathrm{d}t' \tag{6}$$

where the memory function is

$$M(t-t') = -\frac{\mathrm{d}\, G(s)}{\mathrm{d}\, s} = mc(t-t')^{-(m+1)} \tag{7}$$

where $s = (t-t')$, and the damping function $h(\gamma)$ is given by

$$h(\gamma) = \frac{1}{1 + \frac{\xi'}{3}\gamma^2}. \tag{8}$$

The parameter ξ' decreased by polydispersity and by long chain branching (Larson, 1985b) and was observed to vary from 0.13 to 0.60 for different polymers (Larson, 1985a;

Table 1
Model parameters for common corn starch (na—not accessible experimentally)

(%)	c (Pa s^m)	m	ξ'
2	0.05	0.78	1.50
4	0.23	0.68	1.59
6	0.43	0.66	0.26
8	0.99	0.61	na

Laun, 1978; Papanastasiou et al., 1983; Soskey & Winter, 1983).

For shear flow, the Finger tensor is given as

$$B(t,t') = \begin{bmatrix} 1+\gamma^2 & \gamma & 0 \\ \gamma & 1 & 0 \\ 0 & 0 & 1 \end{bmatrix} \tag{9}$$

$$\mathrm{I}_B = \mathrm{tr}\, B = 3 + \gamma^2$$

$$\mathrm{II}_B = \tfrac{1}{2}(\mathrm{I}_B^2 - \mathrm{tr}\, B^2) = 3 + \gamma^2$$

$$\mathrm{III}_B = \det B = 1.$$

For steady shear flow starting at time $t = 0$,

$$\gamma(t-t') = \begin{cases} \dot\gamma(t-t'); t' > 0 \\ \dot\gamma t; t' \le 0 \end{cases}. \tag{10}$$

The material function $\eta^+(\dot\gamma, t)$ evaluated using Eq. (6) is given by

$$\eta^+(\dot\gamma,t) = \frac{ct^{1-m}}{\left(1+\dfrac{\xi'(\dot\gamma t)^2}{3}\right)} + mc(\dot\gamma)^{m-1}\int_0^{\dot\gamma t} \frac{\gamma^{-m}}{\left(1+\dfrac{\xi'\gamma^2}{3}\right)}\,\mathrm{d}\gamma. \tag{11}$$

The steady shear viscosity is then given by Larson (1985b)

$$\eta(\dot\gamma) = \lim_{t\to\infty}[\eta^+(\dot\gamma,t)] = \frac{mc\pi}{2\sin[(1-m)\pi/2]}\left(\frac{3}{\xi'}\right)^{(1-m)/2}(\dot\gamma)^{m-1}. \tag{12}$$

Table 2
Model parameters for waxy starch (na—not accessible experimentally)

(%)	c (Pa s^m)	m	ξ'
2	0.21	0.63	0.84
4	0.69	0.59	0.24
6	1.41	0.57	na
8	3.12	0.48	na

Stress relaxation modulus is then given as

$$G(t) = ct^{-m} \tag{13}$$

$$G(\gamma,t) = ct^{-m}\left(\frac{1}{1+\dfrac{\xi'}{3}\gamma^2}\right). \tag{14}$$

The storage modulus (G') and the loss modulus (G'') are given by Larson (1985b)

$$G' = \omega\int_0^\infty G(t)\sin\omega t\,\mathrm{d}t = \frac{c\pi\omega^m}{2\Gamma(m)\sin(m\pi/2)} \tag{15}$$

$$G'' = \omega\int_0^\infty G(t)\cos\omega t\,\mathrm{d}t = \frac{c\pi\omega^m}{2\Gamma(m)\cos(m\pi/2)} \tag{16}$$

where $\Gamma(m)$ is the gamma function.

The values of c and m were obtained from nonlinear regression on stress relaxation data within the linear viscoelastic regime using Eq. (13) as the regression function. The parameter ξ' was then evaluated from Eq. (12) by nonlinear regression on experimental steady shear viscosity data. The values of the three parameters c, m, and ξ', obtained for different concentrations of common corn and waxy starch, are given in Tables 1 and 2, respectively. High amylose starch solutions were in the semi-dilute concentration regime, and the dilute solution theory was not applicable.

3. Results and discussion

The method of preparation was finalized based on the ability to get repeatable data for samples prepared at different times. Dintzis and Bagley (1995a) noted that even at low concentrations of 2%, there was uncertainty of the extent of dispersion of the starch, and there might be microscale concentration fluctuations. Similar local inhomogeneties were observed visually for the starch samples used in this study. Once the starch samples were prepared, varying storage time had no effect on rheological properties. However, if the stirring time was increased during sample preparation, the rheological properties changed. As a representative example, shear moduli for 6% waxy starch decreased with increase in stirring time to 20 min during sample preparation. This is depicted in Fig. 1. It was concluded that starch samples were stable in 90% DMSO-10% water, but rheological properties were a function of the sample preparation methodology.

The values of c, m, and ξ' (Eq. (14)) were used in the K-BKZ model to predict the various material functions in shear for waxy and common corn starch. The parameter c is a measure of the strength of a critical gel (Izuka, Winter & Hashimoto, 1992). The value of c increases with increasing concentration for common corn starch and waxy starch as expected (see Tables 1 and 2). The value of m decreases with increasing entanglements, as borne out by the decreasing

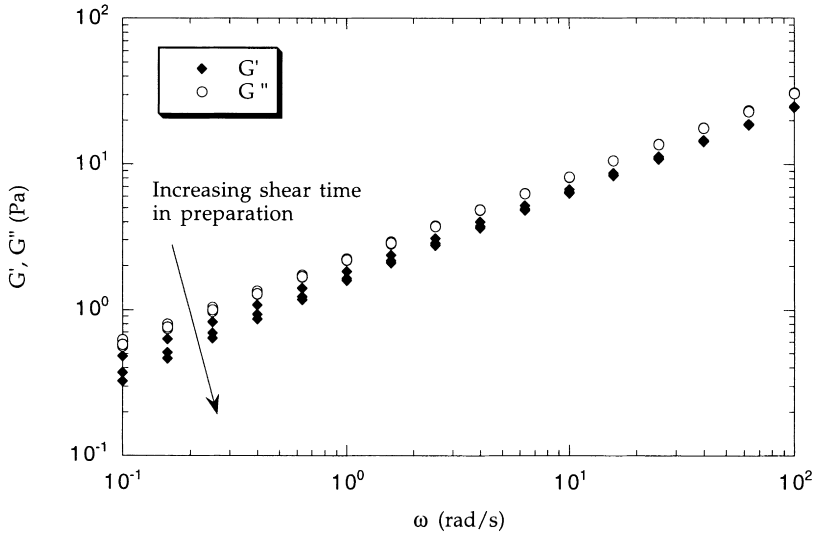

Fig. 1. Effect of increasing shear on dynamic properties of 6% waxy starch.

value of m with increasing concentration in Tables 1 and 2. The slope of the G' and G'' vs. freq. lines on a log–log scale is the parameter m for a critical gel. Two values of m are obtained, one from the G' curve and the other from the G'' curve, but these two values should be the same for a critical gel. From Table 3, the slope for 6% common corn starch is 0.65 and 0.63 (G' and G''), and 0.57 and 0.56 for 6% waxy starch. Comparing these values to the value of m obtained from stress relaxation data given in Tables 1 and 2, indicates a value of 0.66 for 6% common corn, and 0.57 for 6% waxy starch. The slopes of the G' and G'' curves (Table 3) are not expected to be the same for the other "non-critical" gels.

3.1. Dynamic properties

The dynamic properties are summarized in Table 3 in terms of intercept and slopes of G' and G'' vs frequency on logarithmic plot. The constitutive equation overpredicted G'' data for 2% concentration common and waxy corn starch for frequency greater than 1 rad/s. G' and G'' values predicted by Eqs. (15) and (16) for 4, 6, and 8% concentration common corn starch and 4 and 6% waxy corn starch were within 5% of the experimental data over the frequency range investigated. A crossover was observed in the experimental G' and G'' data for 8% waxy starch. The model was derived on the assumption of a constant tan δ value, and thus dynamic data for 8% waxy starch at frequency greater than 10 rad/s were underpredicted.

Strictly speaking, Eqs. (15) and (16) are valid for critical gels only. Critical gels are formed for 6% common corn starch (tan δ vs. ω plot is flat), and for 6% waxy starch (again tan δ vs. ω plot is flat). One of the consequences of using a critical gel equation is that an infinite relaxation time (since a critical gel has an infinitely long relaxation time) is implicitly assumed. These equations have been used to model the other "near-critical" concentrations also as power-law behavior dominates in that regime. However, on moving away from the critical gel concentration, there is in fact a distribution of relaxation times as borne out by the G' and G'' vs. freq. curves which move away from parallel with increasing freq. This leads to the higher deviation from the model prediction as freq. increases. The reason the prediction matches well with experimental data at freq. less than 1 rad/s is because in that regime of freq. the longest relaxation time dominates which is exactly what the model is based on, i.e. infinite relaxation time.

Table 3
Slope (n) and intercept (A has units of Pa s^m) of log G' vs log ω and log G' vs log ω plots

Concentration (%)	High amylose corn starch				Common corn starch				Waxy corn starch			
	G'		G''		G'		G''		G'		G''	
	A	n	A	n	A	n	A	n	A	n	A	n
2	9×10^{-4}	1.29	0.019	0.89	0.076	0.76	0.16	0.69	0.26	0.63	0.37	0.57
4	6×10^{-3}	1.08	0.054	0.90	0.31	0.67	0.54	0.64	0.89	0.59	1.18	0.56
6	0.02	0.98	0.12	0.88	0.60	0.65	0.96	0.63	1.82	0.57	2.25	0.56
8	0.03	0.99	0.20	0.87	1.34	0.61	1.92	0.63	4.01	0.49	3.87	0.54

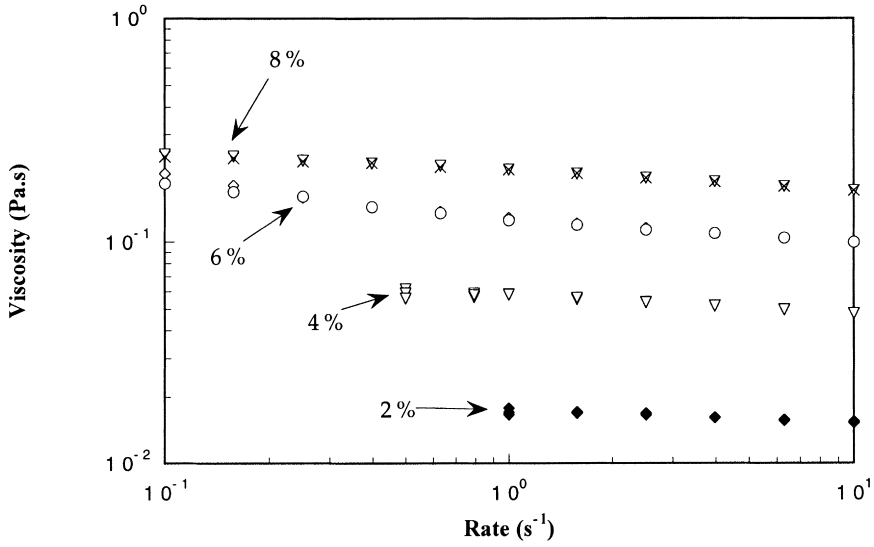

Fig. 2. Variation of shear viscosity with concentration and shear rate for high amylose starch. Numbers denote concentration in % w/v.

3.2. Steady shear measurements

3.2.1. Effect of concentration

Steady shear data for high amylose starch are depicted in Fig. 2. Multiple points represent replicate runs. Low torque signal becomes limiting at low shear rates. Zero shear viscosity increases with increasing concentration. The decrease in viscosity with increasing shear rate is small. The onset of shear thinning occurs at a lower shear rate with increasing concentration. This could be due to the onset of entanglements caused by the presence of the highly branched, high molecular weight amylopectin. The non-Newtonian behavior observed with increasing concentration, as manifested by the decrease in the power-law index (see Table 3), could be attributed to the onset of entanglements.

Steady shear data for common corn and waxy starch are depicted in Figs. 3 and 4, respectively. Multiple points represent replicate runs. Solid lines are fits to experimental data to determine ξ' from Eq. (12). Reproducible data could not be obtained for 8% common corn starch, and 6% and 8%

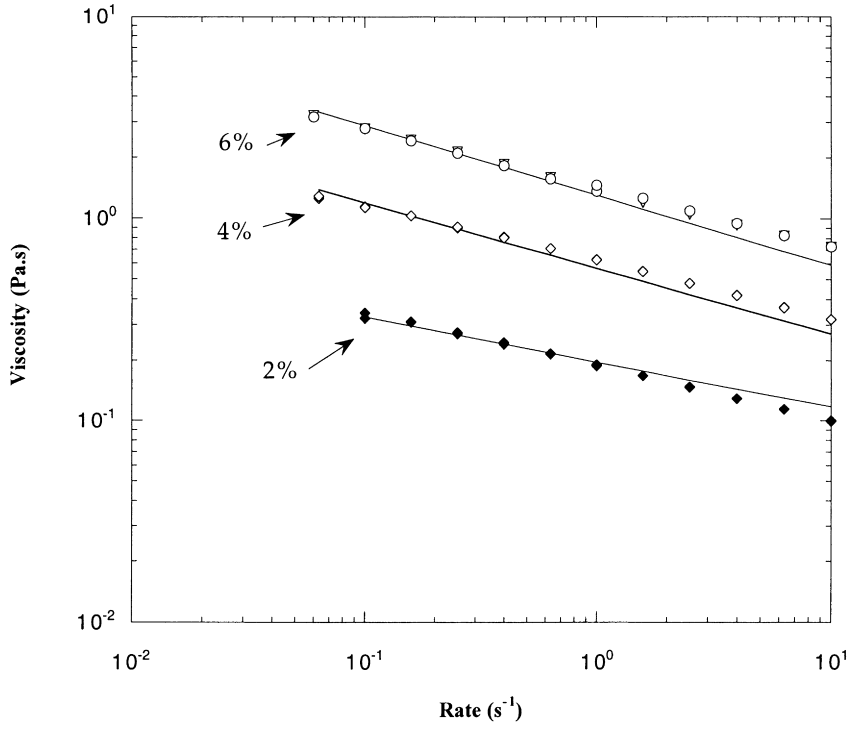

Fig. 3. Variation of shear viscosity with concentration and shear rate for common corn starch: Lines are fits to data to determine ξ' from Eq. (12).

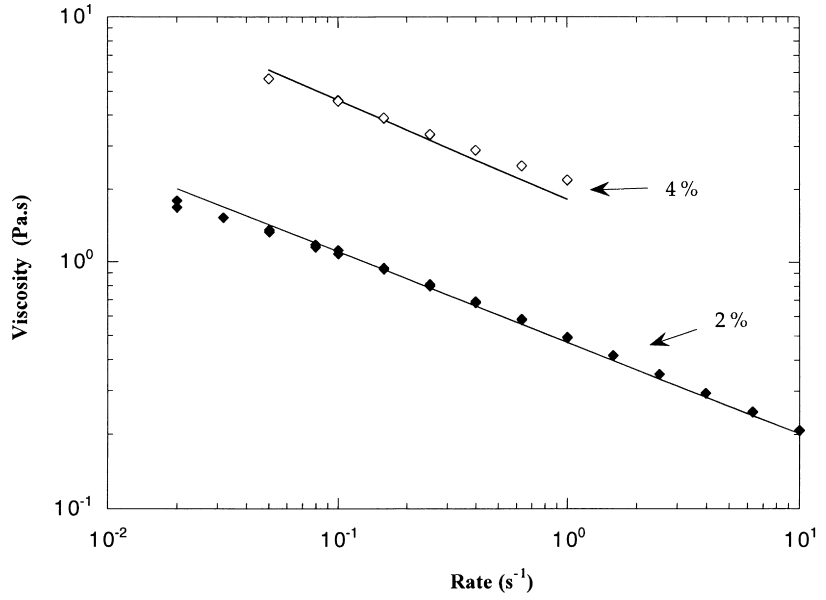

Fig. 4. Variation of shear viscosity with concentration and shear rate for waxy starch. Lines are fits to data to determine ξ' from Eq. (12).

waxy starch. These samples were critical gels or viscoelastic solids as was concluded from dynamic data in the linear viscoelastic regime (Kapoor, 1998). The nonlinear viscoelastic properties of these three samples were observed to be very sensitive to the method of preparation. Network rupture occurred above a certain strain magnitude, and steady state was not attained in transient shear experiments for 8% common corn, and 6 and 8% waxy starch. For the other samples, viscosity increased with increasing concentration. Shear thinning behavior was observed throughout the range of shear rates studied and could be attributed to stress-induced breakdown of the network (Venkataraman & Winter, 1990). The phenomena of shear-thickening and flow induced structure were not observed in this study, due to the shear rate regime in this work ($<10\ s^{-1}$). Odd effects have been reported at higher shear rates (Dintzis & Bagley, 1995a,b; Dintzis et al., 1996), and there could be potential problems in shear rate regimes $>20\ s^{-1}$.

3.2.2. *Effect of starch composition*

Viscosity of waxy starch was higher by a factor of approximately 100 from high amylose starch at similar concentrations and shear rates. High amylose starch exhibited shear thinning at higher concentrations, as compared to

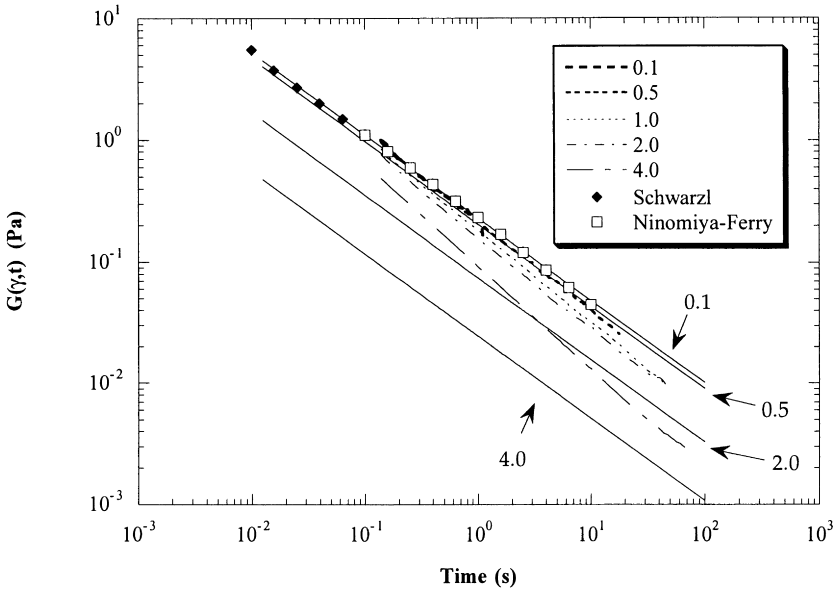

Fig. 5. Stress relaxation upon step strain for 4% common corn starch. Numbers denote strain magnitude. Symbols represent data from LVE interrelations. Solid lines are predictions from Eq. (14).

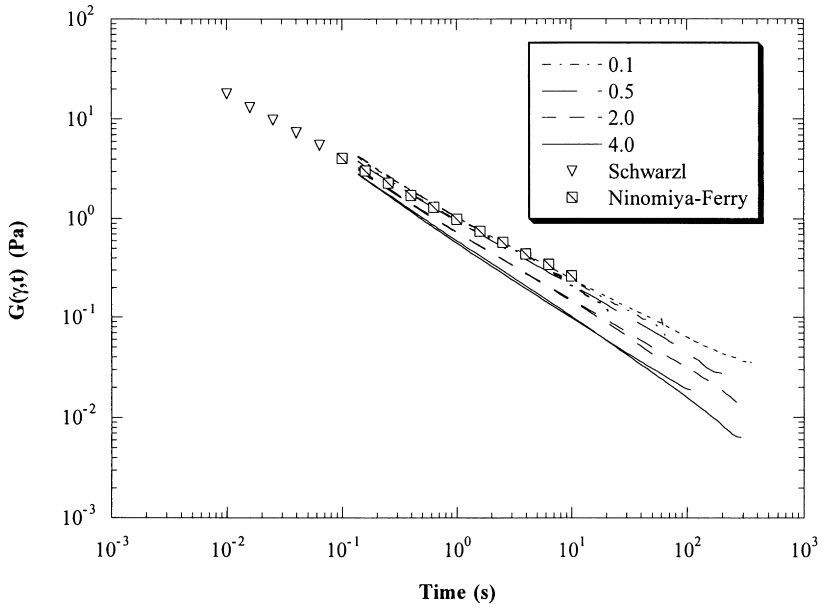

Fig. 6. Stress relaxation upon step strain for 8% common corn starch. Numbers denote strain magnitude. Symbols represent data from LVE interrelations.

waxy and common corn starch, where shear thinning was observed at the lowest concentration studied. These differences could be explained on the basis of the higher amylopectin content in common corn and waxy starch, with the formation of a network due to physical crosslinks, as compared to the semidilute solution behavior of high amylose starch.

3.3. Transient shear measurements

3.3.1. Stress relaxation after step strain

Stress relaxation moduli for 4% common corn starch are depicted in Fig. 5. Similar behavior was observed for the other concentrations. Transducer inertia affects data at short time, and causes deviation from LVE transformations for

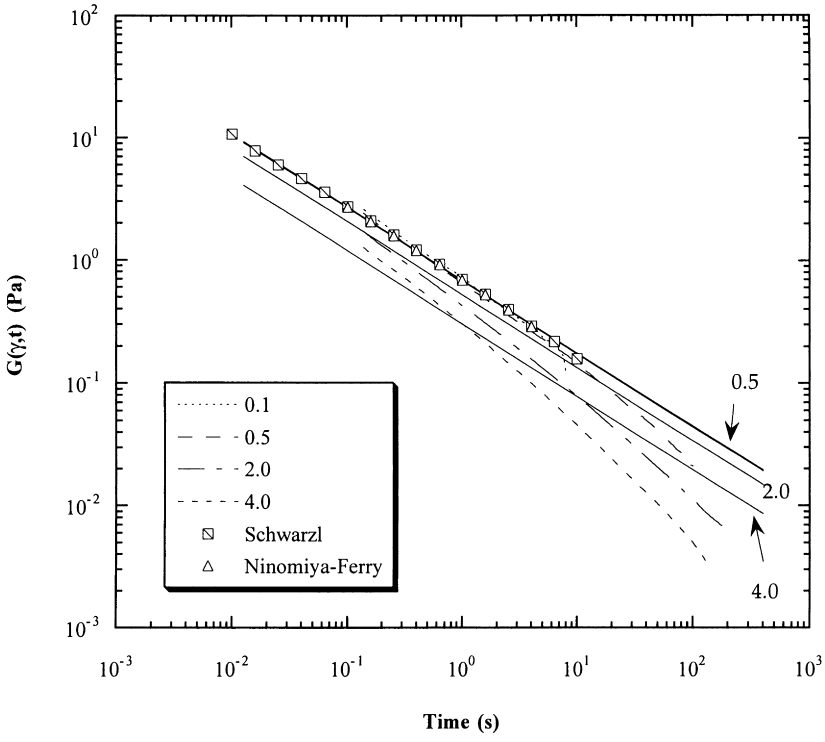

Fig. 7. Stress relaxation upon step strain for 4% waxy starch. Numbers denote strain magnitude. Symbols represent data from LVE interrelations. Solid lines are predictions from Eq. (14).

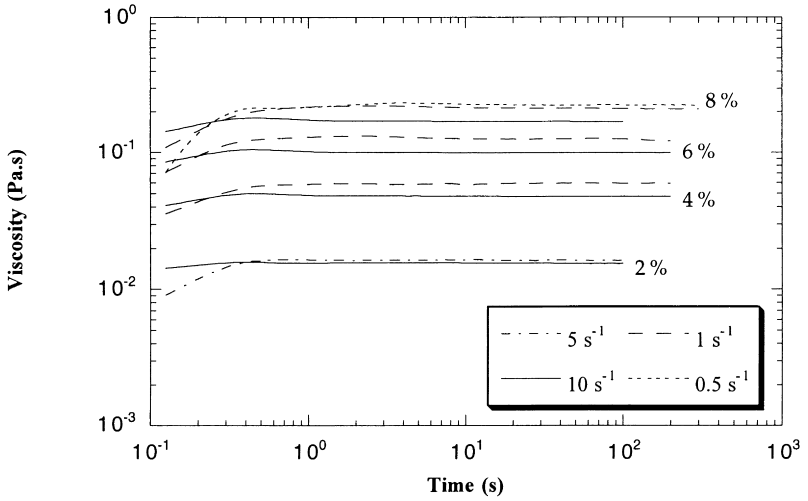

Fig. 8. Viscosity growth upon startup of shear for high amylose starch. Numbers denote steady shear rate.

time less than about 0.1 s. Low torque signal and transducer hysteresis affect data at long time. Solid lines in the figures are predictions from a single integral constitutive equation (Eq. (14)). Stress relaxation moduli for common corn starch for step strain value of 0.1 are observed to agree with the prediction from the Schwarzl and Ninomiya–Ferry relations for time greater than 0.1 s. This was consistent with the expectation that $G(\gamma,t)$ must reduce to the linear viscoelastic modulus $G(t)$ for small strains. For higher strain values, the curves were shifted down. The shape of the relaxation moduli curves in the range of valid data suggested the applicability of time-strain separability for 2 and 4% common corn starch. Nonlinear behavior with increasing strain magnitude was overpredicted by Eq. (14) for 2 and 4% common corn starch. Strain softening was underpredicted for 6% common corn starch. A more complex behavior was observed for 8% common corn starch, where increase of the step strain to a magnitude of about two led to poor reproducibility of data for successive runs with the same sample. Data shown in Fig. 6 were generated by using a fresh sample for each step strain experiment. Time-strain separability does not appear to hold for 8% common corn starch, and the assumption of time-strain separability in the case of 6% common corn starch was an approximation.

The interconversion of material functions in the linear viscoelastic regime allowed the mapping of material functions in time scale otherwise experimentally inaccessible or dominated by instrument and/or sample limitations, using appropriate transformations on data obtained from other experiments. For example, stress relaxation data were obtained using linear viscoelastic transformations on data from stress growth and sinusoidal oscillations experiments by Meissner (1972), using the method of Schwarzl (1970) given as

$$G(t) = \{G'(\omega) - 0.566G''(\omega/2) + 0.203G''(\omega)\}_{\omega=1/t}. \quad (17)$$

Another transformation method was that of Ninomiya and Ferry (Ferry, 1980) given as

$$G(t) = \{G'(\omega) - 0.40G''(0.40\omega) + 0.014G''(10\omega)\}_{\omega=1/t}. \quad (18)$$

Eqs. (17) and (18) were used to convert experimental dynamic material function data to stress relaxation data. The predictions from the Schwarzl relation were in agreement with those from the Ninomiya–Ferry relation and extended the time scale to about 0.01 s. Mismatch between LVE transformations and experimental data below about 0.1 s led to the conclusion that instrument effects dominated at short time for high amylose starch. At time greater than about 0.2 s, low torque signal and transducer hysteresis affected data for high amylose starch.

Stress relaxation moduli for 4% waxy starch are depicted in Fig. 7. Data at short time (<0.1 s) were dominated by instrument effects, as observed from the deviation from LVE transformations. Low torque signal and transducer hysteresis affect data at long time. Solid lines in the figures are predictions from a single integral constitutive equation (Eq. (14)). Curves for step strain magnitudes of 0.1 and 0.5 compare well for 2 and 4% waxy starch, with stress relaxing to zero for all the strain magnitudes. Time-strain separability appears to be applicable in the range of valid data for 2 and 4% waxy starch. Data for 6 and 8% waxy starch were extremely sensitive to method of preparation and magnitude of strain applied. Reproducible data sets could not be obtained for step strain magnitudes outside the LVE regime, even though a fresh sample was used for each experimental run. For 6 and 8% waxy corn starch, repeated runs with strain magnitude greater than 0.1 led to variation in the viscoelastic behavior from sample to sample. For 2 and 4% waxy corn starch, nonlinear behavior with increasing strain magnitude was underpredicted for time greater than 1 s by Eq. (14). Time-strain separability does not seem to be

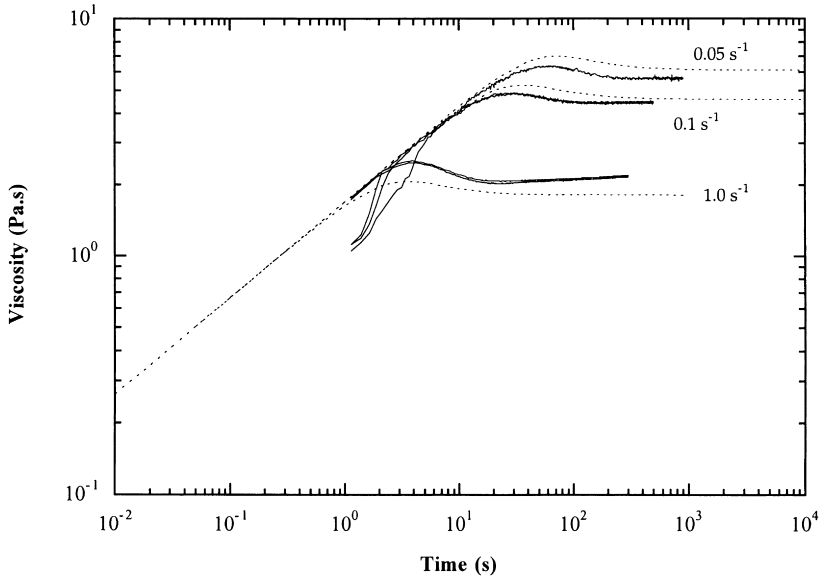

Fig. 9. Viscosity growth upon startup of shear for 4% waxy starch. Numbers denote steady shear rate. Dashed lines are predictions from Eq. (11).

applicable for 6 and 8% waxy starch. The curves for 8% waxy starch flatten out at long times, indicating the existence of an equilibrium modulus G_e, typical of a viscoelastic solid. The magnitude of G_e for 8% waxy starch was estimated to be about 0.3 Pa, as determined by the long time portion of the stress relaxation modulus curve for a step strain magnitude of 0.1.

3.3.2. Stress growth upon startup of steady shear flow

Stress growth material function $\eta^+(\dot{\gamma}, t)$ upon startup of steady shear flow is plotted in Fig. 8 for the four concentrations of high amylose starch. Data are shown for shear rates of 5 and 10 s^{-1} for the 2% sample, 1 and 10 s^{-1} for the 4 and 6% samples, and 0.5, 1 and 10 s^{-1} for the 8% sample. Steady state was attained within 1 s. Non-Newtonian behavior was observed for concentrations greater than 2%. Bird et al. (1987) observed that shear stress approached its steady state value monotonically only for very small shear rates. For shear rate values in the linear viscoelastic regime, steady state viscosity is independent of the shear rate. However, for shear rate values outside the linear viscoelastic regime, an initial stress overshoot is typically observed for polymeric materials before the attainment of steady state, with the steady state value decreasing with increasing shear rate. Deviations from linear viscoelastic behavior are typically observed above a certain strain value. Thus, nonlinear effects are observed at smaller time with increasing shear rate.

The above observations were consistent with data for 2, 4 and 6% common corn starch. The predictions for startup of steady shear by the single integral constitutive equation (Eq. (11)) were within 5% of experimental data, with a stress overshoot predicted for increasing shear rate. A stress overshoot was observed for common corn and waxy starch, with the magnitude of overshoot increasing with shear rate. For the 2% common corn starch sample, low torque signal contributed to scatter in viscosity data. For time less than about 3 s, the curves do not overlay. This was contrary to the expected behavior in the LVE regime, as deviation from the linear viscoelastic curve occurs only above a certain strain value. In the range of concentrations investigated, the curve for shear rate of 1.0 s^{-1} was higher than the curves for lower shear rates at time less than about 3 s. There is a finite time interval between the startup of rotation of the outer cup and the attainment of steady flow field at the transducer surface (inner bob). There are two contributions to the rise time, one being the time taken to develop the velocity profile in the annulus, the other being the time taken by the torque signal to rise above the detection limit of the transducer. It takes longer for the requisite level of torque to be established at the transducer surface at lower shear rates where the transducer sensitivity dominates. This finite rise time combined with the effect of transducer inertia is the cause of the lack of agreement at short time amongst the curves for $\eta^+(\dot{\gamma}, t)$ at different shear rates. The nonlinear properties of 8% common corn starch could not be predicted using the K-BKZ model as the parameter ξ' was not accessible experimentally due to lack of reproducible steady shear viscosity data.

The growth of viscosity upon startup of steady shear for 4% waxy starch is depicted in Fig. 9. Multiple lines represent replicate runs. A stress overshoot was observed, with the magnitude of overshoot increasing with increasing shear rate. Similar behavior was observed for 2% waxy starch data except that the stress overshoot was less prominent. There was a lack of overlap among the curves for time $t < 3$ s, similar to that observed for common corn starch. The dashed lines shown in the figures are predictions for startup of steady shear from Eq. (11). Viscosity growth predictions were within 5% of experimental data for 2% waxy starch,

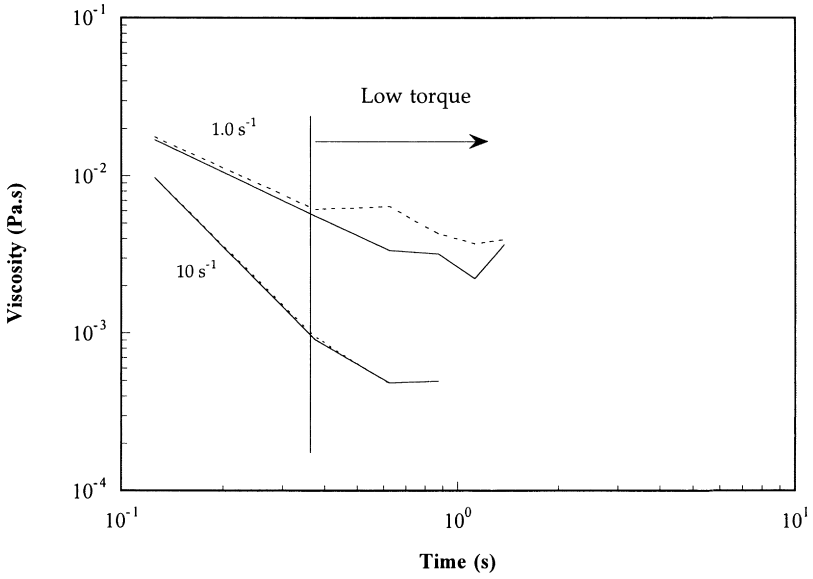

Fig. 10. Stress relaxation upon cessation of shear for 4% high amylose starch. Replicate runs shown. Torque decays below transducer sensitivity within 1 s.

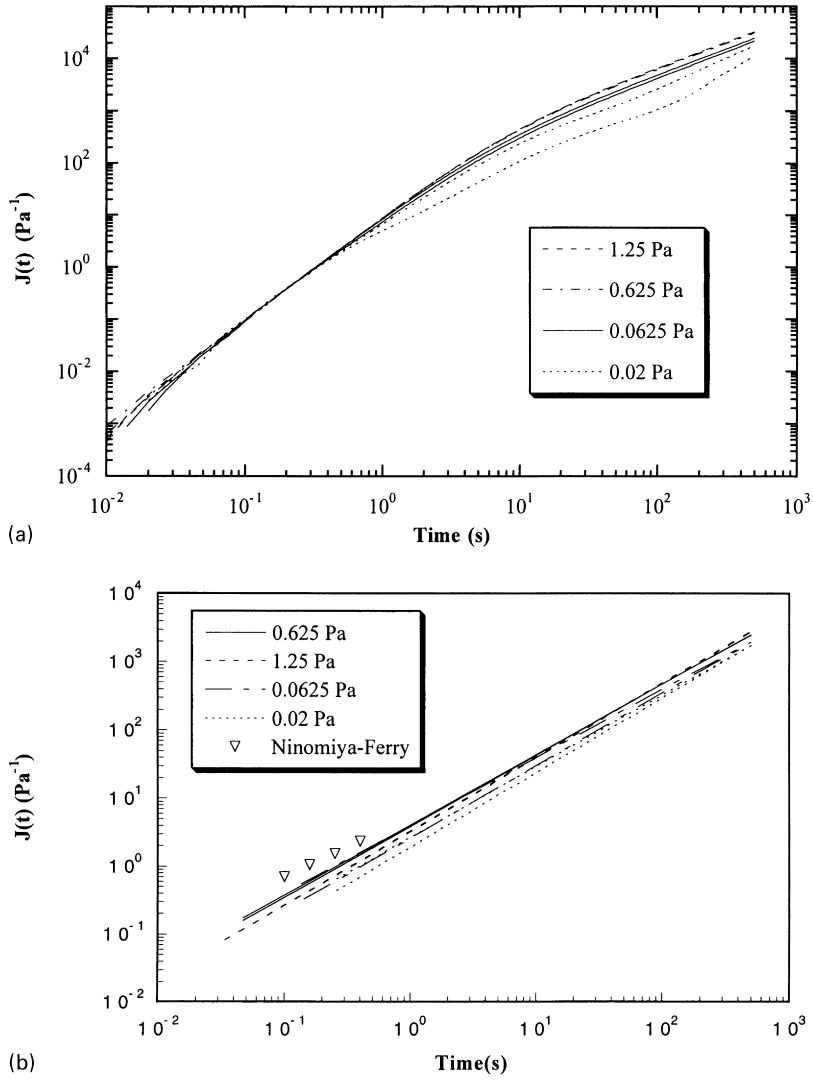

Fig. 11. (a) Creep compliance data for 2% high amylose starch. (b) Creep compliance data for 8% high amylose starch. Symbols are predictions from Eq. (19).

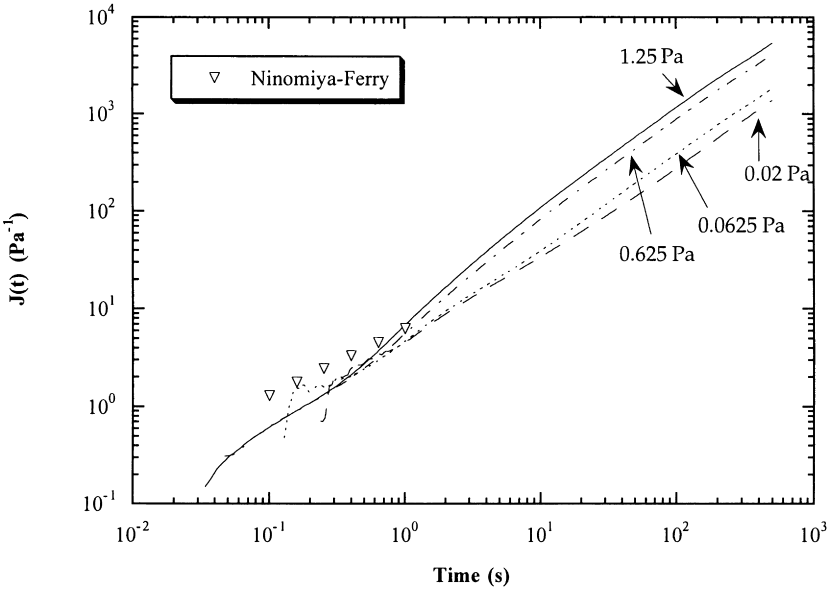

Fig. 12. Creep compliance data for 2% common corn starch. Symbols are predictions from Eq. (19).

with a stress overshoot predicted for increasing shear rate. However, the deviation observed at a shear rate of 1.0 s^{-1} for 4% waxy starch was due to the difference between the regression function and the steady shear viscosity experimental data.

A more complex behavior was observed for 8% common corn and 6% and 8% waxy starch. There was a remarkable lack of reproducibility in data for these compositions. A fresh sample was used for each run, taking care to minimize variation in preparation method. The lack of overlap after about 40 s could be attributed to rupture of the network at an estimated strain magnitude of two units. For 6% waxy starch, each run approached a different plateau value. The lack of overlap for 8% waxy starch runs, and nonlinear effects appear at an estimated strain magnitude of two. Similar observations have been reported for crosslinking polymers near the gel point, and were attributed to network rupture above a certain strain magnitude (Venkataraman & Winter, 1990). Amylose has a helical conformation in DMSO based on a review of relevant work in the literature (Kapoor, 1998). The hydrodynamic conformation of amylopectin has been reported as a disk-like oblate ellipsoid (Callaghan & Lelievre, 1985; Lelievre, Lewis & Marsden, 1986). Therefore, there is a mixture of helical and non-helical conformations in this study. Dynamic moduli data indicate formation of self similar clusters at higher concentrations

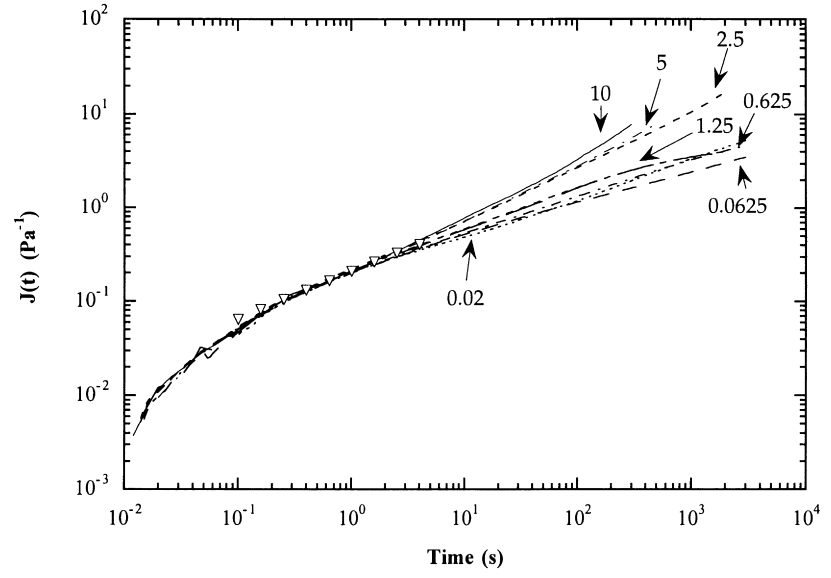

Fig. 13. Creep compliance data for 8% waxy starch. Numbers denote applied stress in Pa. Symbols are predictions from Eq. (19).

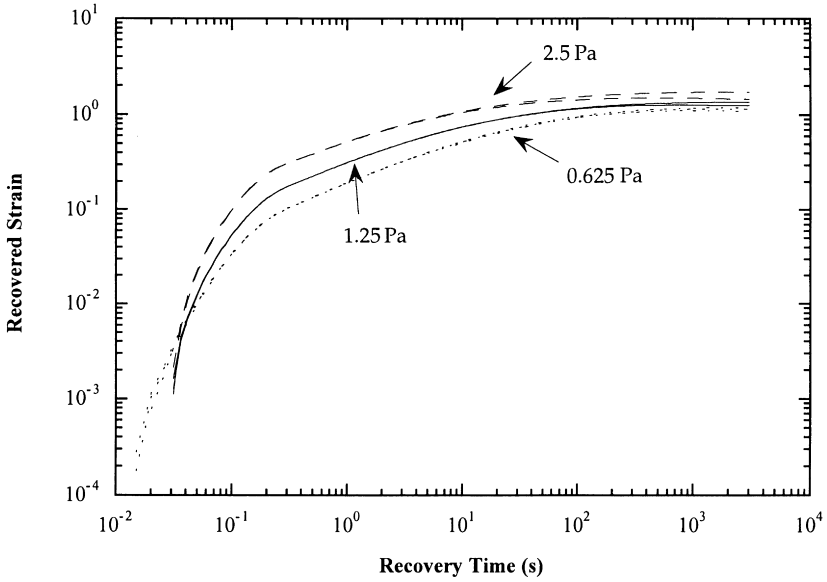

Fig. 14. Recovery curves for 8% common corn starch.

for these starch samples (Kapoor, 1998; Kapoor & Bhattacharya, 2000). Due to lack of reproducible steady shear viscosity data, the parameter ξ^{l} was not accessible experimentally for 8% common corn and 6% and 8% waxy starch. Consequently, nonlinear properties could not be predicted for these samples.

3.3.3. Stress relaxation after cessation of steady shear flow

Data for stress decay upon cessation of steady shear flow are depicted as $\eta^{-}(\dot{\gamma}, t)$, in Fig. 10 for 4% high amylose starch. Data for 2% high amylose starch was not experimentally accessible due to torque being below the limit of transducer sensitivity. Low torque signal affected data for high amylose starch. Torque magnitude decayed to less than 0.002 g cm within 1 s for high amylose starch. Stress also relaxed monotonically to zero with the relaxation being more rapid for higher values of the preceding shear rate. Stress relaxed monotonically to zero for common corn starch solutions of different concentrations with the relaxation being more rapid for higher values of the preceding shear rate. Similar observations were valid for 2% and 4% waxy starch.

3.3.4. Creep and recovery measurements

Creep compliance data were obtained for 2 and 8% high amylose starch and are depicted in Figs. 11a and b. Numbers denote the applied stress in Pa. The open symbols depicted in Figs. 11b, 12 and 13 are data from linear viscoelastic transformations on data from sinusoidal oscillations experiments, using the method of Ninomiya and Ferry (Ferry, 1980) given as

$$J(t) = \{J'(\omega) + 0.40J''(0.40\omega) - 0.014J''(10\omega)\}_{\omega=1/t}. \quad (19)$$

Magnitude of instrument effects could be estimated by the difference between experimental data and LVE transformations. The predictions from the Ninomiya–Ferry relation are higher than the experimental data in Figs. 11b and 12 because instrument effects dominated at short times (<1 s). Scatter in $J(t)$ data was observed until a time of about 1 s. Low torque signal caused the lack of reproducibility observed for 2% high amylose starch at an applied stress of 0.02 Pa. $J(t)$ data for both concentrations of high amylose starch appeared to be in the nonlinear regime as evidenced by the lack of overlap for different stress magnitudes. However, data obtained were typical of a viscoelastic liquid, with the attainment of a steady shearing flow at long time. Rheometrics instrument software was used to detect the presence of a steady shearing flow. The software divided the creep compliance curves into equal sized windows of data. A linear least squares regression was performed for each window, starting from the end of the curve and working towards time zero. Steady state was detected when the difference between slopes of adjacent windows was less than a specified value, termed the slope tolerance. The number of windows and the slope tolerance could be specified by the user, and had values of 10 and 10%, respectively, in this analysis. The value of the equilibrium compliance J_{e0} was calculated by extrapolating the line resulting from the linear regression in the steady state window to $t = 0$. The value of the equilibrium compliance would be the true J_{e0} value if the analysis is in the LVE regime. This was not the case of high amylose starch, and the J_{e0} value is not reported.

Creep compliance data for common corn starch are depicted in Fig. 12. The LVE limit for the applied stress could not be determined due to the lack of overlap observed in the $J(t)$ curves. 2% common corn starch attained steady state flow at long time, as detected by instrument software. An average value of 7.34 for J_{e0} was obtained for 2%

common corn starch from replicate runs at the lowest applied stress of 0.02 Pa. Steady state flow was not attained at long time for 8% common corn starch, typical of a viscoelastic solid. However, repeated runs at the same stress level for the same sample led to the attainment of a steady state flow at long time. Thus a change in viscoelastic behavior from a viscoelastic solid to a viscoelastic liquid was observed for 8% common corn starch. Similar observations have been reported for crosslinking polymers near the gel point (Venkataraman & Winter, 1990) and were attributed to mechanical rupture of the network.

Creep compliance data were obtained for 2, 6, and 8% waxy corn starch. Fig. 13 depicts the data for 8% waxy starch. Instrument effects dominate for time less than 0.5 s for 2 and 6% waxy starch and for time less than 0.2 s for 8% waxy starch. Applied stress magnitude less than 0.0625 Pa were in the LVE regime for 2% waxy starch. Increasing stress magnitude greater than 0.0625 Pa led to nonlinear behavior. 2% waxy starch attained steady state flow at long time, typical of a viscoelastic liquid. An average value of 8.77 Pa^{-1} for J_{e0} was obtained for 2% waxy starch from replicate runs at the lowest applied stress of 0.02 Pa.

Increasing stress magnitude above 0.625 Pa led to nonlinear behavior for 6% waxy starch. Steady state flow was attained at long time for 6% waxy starch, typical of a viscoelastic liquid. Dynamic data had led to the conclusion that 6% waxy starch was a critical gel. Venkataraman and Winter (1990) observed that a steady state flow was not attained for critical gels. However, an increase in the magnitude of applied stress was reported to cause a change in behavior from a viscoelastic solid to that of a critical gel (Venkataraman & Winter, 1990). Similar behavior was observed for 6% waxy starch, and repeated runs at the same stress level for the same sample led to the attainment of a steady state flow at long time. The LVE limit of applied stress for 8% waxy starch could not be determined due to the lack of overlap observed in the $J(t)$ curves. A steady state flow was not attained for applied stress magnitude less than 1.25 Pa, typical of a viscoelastic solid. Higher magnitude of applied stress led to the attainment of a steady state flow, as in the case of 8% common corn starch and 6% waxy starch, and could be attributed to network rupture effects.

Instrument inertia dominated recovery data for 2 and 8% high amylose starch, as well as 2% common corn starch, despite the use of inertia correction procedures by the instrument software. Instrument inertia effects were observed for time less than 0.1 s for 8% common corn starch, as depicted in Fig. 14. Recovered strain for 8% common corn starch approached a plateau value at long time. The plateau value increased with increasing preceding stress magnitude and was between 1 and 2 strain units. A change in slope was observed in recovered strain curves at about 0.3 s. Recovered strain for waxy starch also approached a plateau value at long time. Inertia effects decreased with increasing sample concentration, as was observed from the short time portion of the recovery curves. The plateau value increased with increasing preceding stress magnitude, and was in the range 0.3–1.0, 2–10, 0.03–10 strain units for 2, 6, and 8% waxy starch. The high magnitude of recovered strain for 6 and 8% waxy starch were typical of a critical gel and viscoelastic solid, where a complete recovery is predicted at infinite time (Venkataraman & Winter, 1990).

4. Conclusions

The effect of starch composition and concentration on steady shear and transient properties of starch in a mixed solvent (10% water-90% DMSO) was investigated. The amylopectin content in the starch increased in the order high amylose starch < common corn starch < waxy starch. The starch samples were stable in the mixed solvent used. However, increasing shear time during sample preparation led to a decrease in shear moduli, consistent with observations reported in the literature (Dintzis & Bagley, 1995a,b; Dintzis et al., 1996). Increasing concentration led to a change in rheological behavior from Newtonian liquid to semidilute solution for high amylose starch, and from semidilute solution to viscoelastic solid for common corn and waxy starch. The amylopectin component of starch has been reported to cause shear thickening and flow induced incipient phase separation at shear rates greater than about 20 s^{-1} (Dintzis & Bagley, 1995a,b; Dintzis et al., 1996). The effects of higher amylopectin content for the same starch concentration was higher shear viscosity and even gel formation (at concentrations of 6 and 8%). This pointed to the formation of networks with increasing amylopectin content. Shear thickening was not observed in this study, which could be due to the shear rate regime used (<10 s^{-1}). A single integral constitutive equation (K-BKZ) gave an acceptable fit to rheological data for 2, 4, and 6% common corn starch, and 2 and 4% waxy corn starch. A more complex rheological behavior was observed for 8% common corn starch and 6 and 8% waxy starch and requires further investigation.

References

Bernstein, B., Kearsley, E., & Zapas, L. (1963). A study of stress relaxation with finite strain. *Transactions of the Society of Rheology*, *7*, 391–410.

Bird, R. B., Armstrong, R. C., & Hassager, O. (1987). *Dynamics of polymeric liquids*. (2nd ed.), vol. 1. New York: Wiley.

Callaghan, P. T., & Lelievre, J. (1985). The size and shape of amylopectin: a study using pulsed-field nuclear magnetic resonance. *Biopolymers*, *24*, 441–460.

Delgado, G. A., Gottnied, D. J., & Ammeraal, R. N. (1991). Maize starch sample preparation for aqueous size exclusion chromatography using microwave energy. In R. B. Friedman, *Biotechnology of amylodextrin oligosaccharides ACS Symposium Series 458* Washington, DC: ACS.

Dintzis, F. R., & Bagley, E. B. (1995a). Shear-thickening and flow-induced structure in a system of DMSO containing waxy maize starch. *Journal of Rheology*, *39* (6), 1399–1409.

Dintzis, F. R., & Bagley, E. B. (1995b). Effects of thermomechanical

processing on viscosity behavior of corn starches. *Journal of Rheology*, *39* (6), 1483–1495.

Dintzis, F. R., & Tobin, R. (1969). Optical rotation of some α-1,4-linked glucopyranosides in the system H_20–DMSO and solution conformation of amylose. *Biopolymers*, *7*, 581–593.

Dintzis, F. R., Berhow, M. A., Bagley, E. B., Wu, Y. V., & Felker, F. C. (1996). Shear-thickening behavior and shear-induced structure in gently solubilized starches. *Cereal Chemistry*, *73* (5), 638–643.

Ferry, J. D. (1980). *Viscoelastic properties of polymers*. (3rd ed.) New York: Wiley.

Izuka, A., Winter, H. H., & Hashimoto, T. (1992). Molecular weight dependence of viscoelasticity of polycaprolactone critical gels. *Macromolecules*, *25*, 2422–2428.

Kapoor, B. (1998). *Rheological properties of starch in aqueous dimethylsulfoxide*. Unpublished MS Thesis, Department of Biosystems and Agricultural Engineering, University of Minnesota.

Kapoor, B., & Bhattacharya, M. (2000). Dynamic and extensional properties of starch in aqueous dimethylsulfoxide. *Carbohydrate Polymers*, *42* (4), 323–335.

Kaye, A. (1962). *College of aeronautics, Cranfield, Note No. 134*.

Krieger, I. M. (1990). The role of instrument inertia in controlled-stress rheometers. *Journal of Rheology*, *34*, 471–483.

Lapasin, R., & Pricl, S. (1995). *Rheology of industrial polysaccharides: theory and applications*, New York: Chapman and Hall.

Larson, R. G. (1985a). Nonlinear shear relaxation modulus for a linear low-density polyethylene. *Journal of Rheology*, *29* (6), 823–831.

Larson, R. G. (1985b). Constitutive relationships for polymeric materials with power-law distributions of relaxation times. *Rheologica Acta*, *24*, 327–334.

Laun, H. M. (1978). Description of the non-linear shear behavior of a low density polyethylene melt by means of an experimentally determined strain dependent memory function. *Rheologica Acta, 17*, 1–15.

Lelievre, J., Lewis, J. A., & Marsden, K. (1986). The size and shape of amylopectin: a study using analytical ultracentrifugation. *Carbohydrate Research*, *153*, 195–203.

Macosko, C. W. (1994). *Rheology: principles, measurements and applications*, New York: VCH.

Meissner, J. (1972). Modifications of the Weissenberg Rheogoniometer for the measurement of transient rheological properties of molten polyethylene under shear. Comparison with tensile data. *Journal of Applied Polymer Science*, *16*, 2877–2899.

Papanastasiou, A. C., Scriven, L. E., & Macosko, C. W. (1983). An integral constitutive equation for mixed flows: viscoelastic characterization. *Journal of Rheology*, *27* (4), 387–410.

Schwarzl, F. R. (1970). On the interconversion between viscoelastic material functions. *Pure and Applied Chemistry*, *23*, 219–234.

Soskey, P. R., & Winter, H. H. (1983). Large step shear strain experiments with parallel-disk rotational rheometers. *Journal of Rheology*, *28*, 625–645.

Venkataraman, S. K., & Winter, H. H. (1990). Finite shear strain behavior of a crosslinking polydimethylsiloxane near its gel point. *Rheologica Acta*, *29*, 423–432.

Wagner, M. H. (1976a). Analysis of stress-growth data for simple extension of a low-density branched polyethylene melt. *Rheologica Acta*, *15*, 133–135.

Wagner, M. H. (1976b). Analysis of time-dependent non-linear stress-growth data for shear and elongational flow of a low-density branched polyethylene melt. *Rheologica Acta*, *15*, 136–142.

Whistler, R. L., & Daniel, J. R. (1984). Molecular structure of starch. In R. L. Whistler, J. N. BeMiller & E. F. Paschall, *Starch: chemistry and technology* (pp. 153–183). Orlando: Academic Press.

Wurzburg, O. B. (1986). *Modified starches: properties and uses*, Boca Raton: CRC.

Young, A. H. (1984). Fractionation of starch. In R. L. Whistler, J. N. BeMiller & E. F. Paschall, *Starch: chemistry and technology* (pp. 249–284). Orlando: Academic Press.